

# U-Capkidnets++-: A Novel Hybrid Capsule Networks with Optimized Deep Feed Forward Networks for an Effective Classification of Kidney Tumours Using CT Kidney Images

J. Sarada<sup>1</sup>, Dr. N.V. Muthu Lakshmi<sup>2</sup>, Dr. T.Lakshmi Praveena<sup>3</sup>

<sup>1</sup> Research Scholar, Department of Computer Science, Sri Padmavathi Mahila Vishva Vidyalayam (SPMVV), Tirupati, Andhra Pradesh – India.

<sup>2</sup> Assistant Professor, Department of Computer Science, Sri Padmavathi Mahila Vishva Vidyalayam (SPMVV), Tirupati, Andhra Pradesh – India.

<sup>3</sup> Department of Computer Science, Sri Padmavathi Mahila Vishva Vidyalayam (SPMVV), Tirupati, Andhra Pradesh – India.

## Abstract:

Chronic Kidney Diseases (CKD) has become one among the world wide health crisis and needs the associated efforts to prevent the complete organ damage. A considerable research effort has been put forward onto the effective separation and classification of kidney tumors from the kidney CT Images. Emerging machine learning along with deep learning algorithms have waded the novel paths of tumor detections. But these methods are proved to be laborious and its success rate is purely depends on the previous experiences. To achieve the better classification and segmentation of tumors, this paper proposes the hybrid ensemble of visual capsule networks in U-NET deep learning architecture and w deep feed-forward extreme learning machines. The proposed framework incorporates the data-preprocessing powerful data augmentation, saliency tumor segmentation (STS) followed by the classification phase. Furthermore, classification levels are constructed based upon the feed forward extreme learning machines (FFELM) to enhance the effectiveness of the suggested model. The extensive experimentation has been conducted to evaluate the efficacy of the recommended structure and matched with the other prevailing hybrid deep learning model. Experimentation demonstrates that the suggested model has showed the superior predominance over the other models and exhibited DICE co-efficient of kidney tumors as high as 0.96 and accuracy of 97.5 % respectively.

**Keywords:** Chronic Kidney Diseases, Machine and Deep learning methods, CT scan Images, Saliency Segmentation, Deep Feed Forward Extreme Learning machines.

## INTRODUCTION:

One of the most promising fields of research is medical image processing (MIP), which aims to extract usable information from enormous data sets. It has gained the most popularity in the medical profession since there is a great need for analytical methodologies for forecasting and locating useful information in health data. The medical industry is producing enormous amounts of complicated data about illnesses, hospitals, treatment procedures, and other topics that need to be processed and analyzed for knowledge extraction. MIP has a variety of intelligent approaches and tools that, when used on this processed data, give professionals the knowledge they need to choose the finest course of technique for enhancing the effectiveness of patient health management duties. For the detection of numerous diseases, including diabetes, skin cancer, kidney cancer, breast cancer, heart disease, kidney malignancies, kidney

stones, liver dysfunction, hepatitis, etc., MIP has a substantial presence in every area of medicine.

Kidney tumors are considered be most deadliest diseases and it is difficult to identify at early stages [1]. Even though it is one of the most lethal cancers, the necessity for early diagnosis of cancer still requires innovation.[2,3] Many types of cancers has overruled the medical community due to the delayed modern methods of diagnosis and treatment. Automatic and intelligent diagnostic tool is required for the doctors for the early diagnosis of this kind of disease which can help the patients for survival. It's challenging to recognise early kidney disease, therefore classification approaches are frequently utilised in many automatic medical diagnostic instruments.[4]. An intelligent method of identifying the kidney cancers can be modelled by data mining techniques. Recently machine learning and deep learning technique is used now days for kidney disease detection. Applications of

machine and deep learning based diagnosis techniques have explored its new light of research to predict the CKD on multiple datasets[5-8]. Common intelligent classifiers which are used in early diagnosis of CKD are listed as : Support Vector Machines(SVM),Naïve Bayes(NB),Decision Trees(DT), Artificial Neural Networks(ANN), Bagging Algorithm, K-nearest neighborhood(KNN) etc. But an accurate segmentation and effective classification of kidney tumors from CT images still needs more improvisation when it is to be deployed for the real time big data analytics.[9,10].

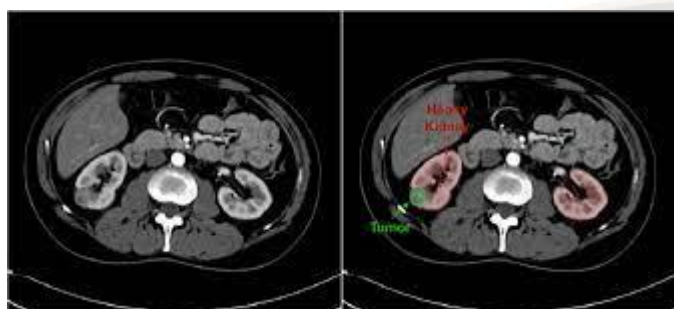


Figure 1 Abnormalities in Kidney CT Scan Images

The major contribution of this research work is as follows

1. Saliency Capsule networks (SCN) was designed to improve the segmentation process and feature extraction capability of the network. The proposed model could effectively strengthen useful features and make full use of the high-level salient feature information to segment the kidney images that aids for the better classification.
2. Combining the capsule networks and U-NET, network structure Modified Capsule U-Net is proposed for the kidney tumour segmentation.
3. Deep Feed Forward Layers based on Extreme Learning Machines are proposed for fully connected networks to achieve the better classification.
4. Completed different Evaluations patterns on the proposed methodology using kidney CT image datasets. At the same time, existing and deep learning methods were selected for comparison and all the experimental results were fully evaluated and analysed. The experimental data shows that our suggested approach worked better than other available models.

**The organization of the paper is as follows as: Section -2**presents the related works by more than one authors. The data collection, data pre-processing, data augmentation and working mechanism of the proposed framework are presented in **Section-3**. The experimental design, implementation methodology, results with comparative analysis is discussed in **Section-4**. Finally the paper is concluded with future scope in **Section-5**.

## Section-2

### Related Works:

G. Chen et al. introduced an efficient and effective Adaptive Hybridised Deep Convolutional Neural Network (AHDCNN) for the early diagnosis of renal disease. By lowering the feature dimension, this framework increased classification system accuracy, and CNN was used to create an algorithm model. The results demonstrate how this framework improved performance in terms of accuracy. In contrast, as the data size grows, the computing complexity also grows [11].

A Support Vector Machine (SVM) classifier is united with a single dimensional deep learning Convolutional Neural Network (CNN) approach that was introduced and developed by N. Bhaskar et al. The condition is identified by tracking the urea levels in saliva. The CNN-SVM integrated network was used, which improved the model's classification precision. With an accuracy of 98.04%, the suggested model correctly identified the samples. But this framework's increased memory usage is considered to be its primary drawback [12].

J. Qin et al. created a perceptron-based integrated scheme for CKD detection that integrates random forest and logistic regression. In order to handle the missing data for each incomplete sample, the K-Nearest Neighbour (KNN) assertion method was utilised, which chooses lots of full samples all comparable dimensions. The average accuracy of this framework was 99.83 percent after 10 runs. However, this framework's increased energy consumption has been identified as its main drawback [13].

The main goal of L. Antony et al. is to put several unsupervised algorithms into practise, assess how well they function, and find the best potential combinations that can boost detection rate and accuracy. This work has used five unsupervised algorithms: K-Means clustering, DB-Scan, I-Forest, and Autoencoder and they have been combined with a variety of feature selection techniques. With the K-Means clustering algorithm and feature reduction techniques combined, clinical data for CKD and non-CKD were classified with an overall accuracy of 99%. The disadvantage of this framework is that it doesn't take the computational complexity of a real-time scenario into account [14].

The objective of D. Pavithra et al. is to employ A Convolutional Neural Network (CNN) to identify CKD from clinical data. Because there are some missing values in the provided data, categorical data is imputed using the most frequent category, and numerical data is imputed using k-nearest neighbours. This framework's key advantage is that it may provide results with great accuracy while just requiring the most basic capabilities. However, training takes a lot of time [15].

A Computed Tomography (CT) scan prediction model based on KNN and an edge detection system was reported by G. S. K. G. Prasad et al. utilising CT scan pictures and blood samples. When a CT or MRI scan is converted into a digital picture, edge detection is a method of image processing which is used to locate specific points or edges. In order to forecast diseases, this model employs the K-Nearest Neighbors (KNN) method. For diagnostic screening, this approach reduces costs and time. For a real-time context, extra resources are needed, albeit [16].

N. Bhaskar et al. created a more effective deep learning model that makes precise predictions by combining a bidirectional Long Short-Term Memory (LSTM) structure with a single-dimensional correlative neural network (1-D CorrNN). In order to use the strengths of both networks in the analysis of time-series data, the LSTM network and neural model are combined. In the testing dataset, this approach had an average accuracy rate of 98.08%. However, while receiving diverse input, classification time is relatively slow [17].

S. Akter et al. used ANN, LSTM, GRU, Bidirectional LSTM, Bidirectional GRU, MLP, and Simple RNN as deep learning algorithms for CKD prediction and classification. Utilizing five alternative methods to extract

and assess characteristics from pre-processed and fitted CKD datasets, these algorithms were deployed based on artificial intelligence. High accuracy of 99%, 96%, and 97% was obtained by simple RNN and MLP, together with a decent prediction ratio and shorter processing time. The increased computing complexity of this system, however, is its principal drawback [18].

An Artificial Neural Network (ANN) model was published by D. Weerasinghe et al. to identify the CKD form based on the physicochemical characteristics of the soil in agricultural regions. The results show that for identifying the illness type, the ANN model exhibits the greatest classification and prediction execution. However, this framework's main drawback is that as data size grows, more energy is consumed [19].

A CKD prediction approach was provided by V. Shanmugarajeshwari et al. employing three deep learning models: optimised CNN, optimised LSTM, and optimised ANN. For the kidney dataset, OCNN was determined to be the best method based on prediction accuracy, with an AUC score of 0.99 and a compilation time of 0.00447 s. The models frequently overfit because to their complex architecture. K-fold cross validation and modernised feature selection approaches are needed to address this problem [20]. Table 1 summarises the pros and cons of the different related works

Author's Name	Proposed methodology	Merits	Demerits
G. Chen et al. [11]	Adaptive hybridized Deep Convolutional Neural Network (AHDCNN)	Patients exploit better and greater affordable healthcare services.	Performance is not stable when increased the data size scale.
N. Bhaskar et al., [12]	convolutional neural network (CNN) and support vector machine (SVM)	High classification accuracy	Require large memory
J. Qin et al., [13]	logistic regression, random forest, KNN	Prediction process is efficient and an economically faster	More energy consumption. Size of the dataset increased, leads to time complexity
L. Antony et al., [14]	K-Means Clustering, DB-Scan, I-Forest, and Autoencoder	Less training time, and high classification accuracy.	High computational complexity in real time scenario
D. Pavithra et a;., [15]	CNN and edge detection system	Required minimum features to provide high accuracy	More time required for training the model
G. S. K. G. Prasad et al., [16]	KNN and edge detection system	Saves time and costs for diagnostic screening	Need additional resources for processing which leads to hardware complexity.
N. Bhaskar et al., et [17]	One dimensional Correlational Neural Network (1-D CorrNN)	Average classification accuracy	Classification speed is low when it receives heterogeneous data.
S. Akter et al., [18]	ANN, LSTM, GRU, Bidirectional LSTM, Bidirectional GRU, MLP, and Simple RNN	High prediction accuracy	Increased computational complexity



D. Weerasinghe et al., [19]	Artificial Neural Network (ANN)	Better prediction performance	More energy consumption. Decrease in a number of features does not ensure Effective classification performance.
V. Shanmugarajeshwari et al., [20]	Optimized CNN, Optimized LSTM and Optimized ANN	Better performance in terms of AUC score and reduced compilation time	Due to complex architecture it leads to overfitting issue.

**Section-3**

**3. System Overview :**

The suggested framework's whole architecture is depicted in Figure 2. The proposed architecture's operational process is divided into four important phases. Image data preprocessing saliency segmentation, Feature extractions followed by deep feed-forward based classification layers.

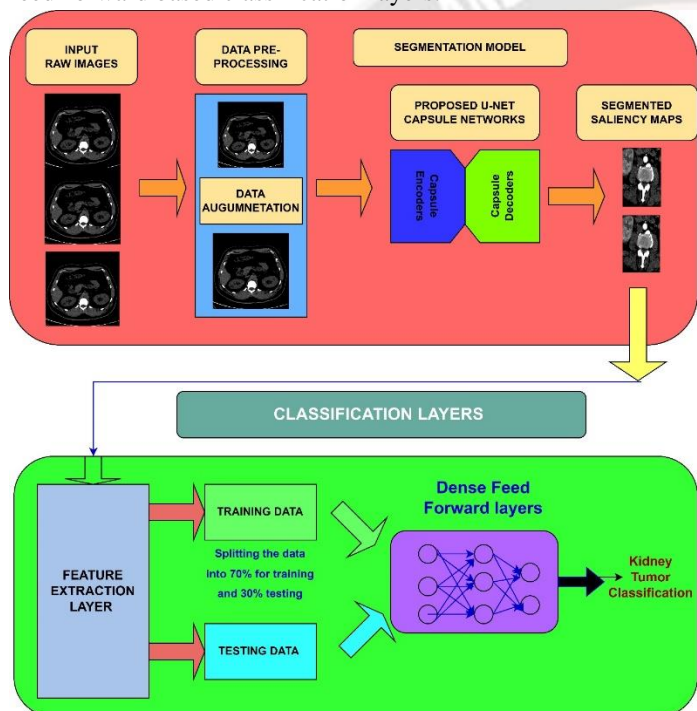


Figure 2 Suggested Framework for the Kidney Tumor Classification

**3.1 Materials and Methods :**

The PACS (Picture archiving and communication system) data were gathered from several hospitals in Dhaka, Bangladesh, where patients had already been diagnosed with kidney stones, cysts, tumours, or normal renal function results. According to the protocol for the whole abdomen, the urogram, and the axial and coronal slices from contrast and non-contrast studies were both chosen. A batch of Dicom images of the region of interest for each radiological finding was then made from the carefully chosen Dicom study, one diagnosis at a time. The Dicom photos were then converted to a lossless jpg image format after we removed each patient's data and meta information. A radiologist and a medical technician double-checked each image finding after conversion to ensure the data was accurate. The generated

dataset contains 12,446 unique data, of which 3,709 are cysts, 5,077 are normal, 1,377 are stones, and 2,283 are tumours.

**3.2 Data Pre-processing:**

With the intention of improving the ability to detect chronic kidney tumours, noise and poor-quality pixels are removed from the data using the data preprocessing technique. The inconsistent pixels and noise pixels from the original kidney ct scan images are removed by the pixel intensive techniques. Additionally, image histogram techniques are used to improve the quality of the photographs because they are more effective with various types of images. The preprocessed CT kidney images are shown in Figure 3 .

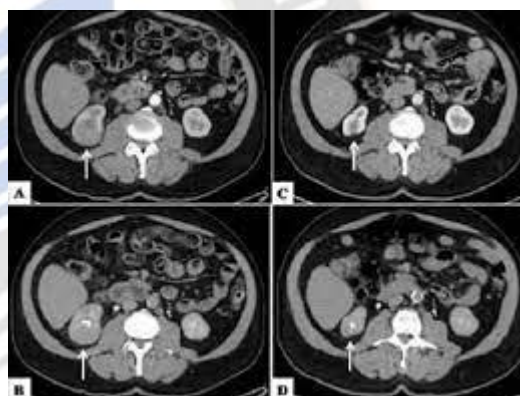


Figure 3 Image Enhancement of CT Kidney Cancer Images used for Classification

After enhancing the images, U-net visual saliency maps are used for an effective segmentation of tumors which are then used for feature extraction and classification.

**3.3 U-Net Based Saliency Maps Segmentation:**

**3.3.1 Saliency Maps –An Overview:**

Segmentation is the process of splitting images into groups using various textures and pixel values. Many techniques have been developed for segmenting the images. Here, a novel technique known as visual saliency maps descriptors has been introduced. It thoroughly breaks down each image into compact, diverse parts. The photographs will be edited to remove any extraneous details.

Color & spatial differences are employed in a pixel based computing, where every pixel is denoted as a block, to generate saliency models[21]. To do this, the pixels "X" are scaled to 256x256, and after that, they are divided into non-

overlying blocks of dimension  $n \times n$ , where  $n=8 \& 16$ . Therefore, the mathematical equations provided by are used to calculate the saliency maps  $M(s)$ .

$$M(s) = \sum_{k=8,16} X(k) * M'(s) \quad (1)$$

As noted in [21], the final saliency maps are derived as the weighted sum of the actual ( $M(s)$ ), previous ( $M(S1)$ ), and next blocks ( $M(S2)$ ) colour and spatial saliency. This is because the position, size, & shape of tumor cells are fairly similar in surrounding clippings.

$$M(s) = w1 * M(m_1) + w2 * M(s) + w * M(s2) \quad (2)$$

Figure 6 shows the saliency maps of kidney cancer images. The refinement of segmentation images requires the use of post-processing techniques once the saliency maps have been calculated. Active contour methods are adapted for all extraction of the saliency counters which leads to the high complexity in terms of computational overhead. To overcome this drawback, this research proposes the U-NET capsule networks for the better contour extraction.

### 3.3.2 Saliency Based U-NET-Capsule networks :

This section discusses about the principle of U-NETs and capsule networks used for the saliency segmentation from the kidney CT scan images.

#### 3.3.2.1 Capsule Networks – An Overview :

Recently, the use of capsule neural networks [22] has been proposed to overcome this drawback of current convolutional neural network . The clusters of neurons known as capsules encode spatial information and the possibility that an object will be present. There is a capsule in the network of capsules that provides the following information for each entity in an image:

1. The possibility that entities exist
2. Parameters for Entity Instantiation

By multiplying the input vectors' matrix by the weight matrix, the necessary spatial connection between the image's low level & high level properties can be encoded as given

$$Y(p, q) = W_{p,q} U(p, q) * S_q \quad (3)$$

In order to select which higher level capsule the current capsule will forward its output to, the weighted input vectors are combined together.

$$S(q) = \sum_q Y(p, q) * D(q) \quad (4)$$

Finally, non-linearity is applied using the squash function. The squashing function maintains the direction of a vector while reducing its length to a maximum of one and a minimum of zero.

$$G(q) = \text{squash}(S(q)) \quad (5)$$

#### 3.3.3.2 Proposed Saliency Segmentation Module :

In first stage, the U-net network is used for the finer segmentation of saliencies from the CT images. U-nets can be categorised essentially into two categories: The initial one is the encoding path, which employs a standard CNN design. Every block in the contracting path has two consecutive  $3 \times 3$  convolutions, a ReLU activation unit, and a capsule layer after them. For effective instruction, this configuration is performed numerous times. The use of the decoder path, which up-samples the feature maps using  $2 \times 2$  up-convolution, is a special feature of the U-net framework. then the upsampled feature outline is mixed with the cropped attribute maps from the relevant layer in the contracting path. Two subsequent layers of the visual capsule and ReLU activation follow this. In order to decrease the feature plans to the necessary digit of channels and create the segmented image,  $1 \times 1$  convolution is eventually applied. The skipping function is adopted to discard the least number of contextual information which results in the segmentation of the image objects from the larger overlapping area. The saliency maps are segmented by using this proposed network and it is extremely useful for a better segmentation of images even it is smaller and also avoids the problem of overfitting. Figure 4 shows capsule based U-NET architecture.

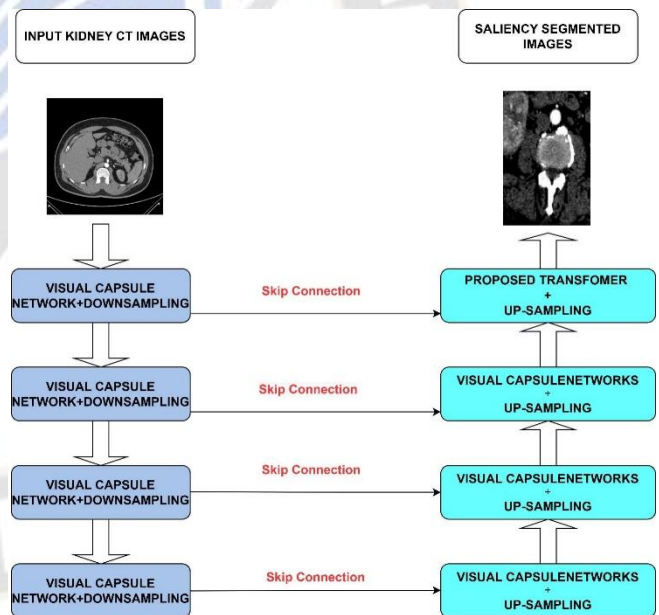


Figure 4 U-NET Framework Used for the Saliency Segmentation

3.4 Feature Extraction Layer :After segmenting the saliency maps, feature extraction layers are formed by capsule networks whose the functionalities are pointed out in the Section 3.2.

#### 3.5 Model Training Layers :

After the feature extracted which are then feed for training the networks. The suggested design substitutes

feedforward networks, which operate on the theory of ELM instead of traditional training network. G.B. Huang proposed the type of neural networks known as Extreme Learning Machines (ELM)[24]. This particular neural network has a hidden layer, for which tuning is not always necessary. ELM performs better, is faster, and has less computational cost than distinct learning algorithms like Support Vector Machines (SVM) & Random Forest (RF)[24].

The kernel function is used by ELM to produce good accuracy and better performance. The ELM's main benefits include less training error & improved estimation. Since ELM employs non-zero activation functions and the automatic tuning of weight biases, it finds usage in classification & its values. The complex workings of the ELM are detailed in [24],[25]. While the activation function of the output layer is inserted directly in this type of system, the "L" neurons in the concealed layer must operate with the stimulation function which is significantly differentiable (ex. the sigmoid function). In ELM, the Hidden layers do not require manual tuning. The loads for the hidden layer are chosen at random. Although it is not entirely accurate to say that concealed nodes are useless, they do not require tuning and their parameters can even be produced at random in advance. Equation (6) gives the system yield for an ELM with a single hidden layer.

$$f_L(x) = \sum_{i=1}^L \alpha_i k_i(x) = k(x)\alpha \quad (6)$$

Where  $x \Rightarrow$  input

$\alpha \rightarrow$  Output weight vector

$$\alpha = [\alpha_1, \alpha_2, \dots, \dots, \dots, \alpha_L]^T \quad (7)$$

$K(x) \Rightarrow$  output concealed layer

$$k(x) = [k_1(x), k_2(x), \dots, \dots, \dots, k_L(x)] \quad (8)$$

The hidden layers are represented by the equation (9) to locate the output vector O, also known as the target vector

$$K = \begin{bmatrix} k(x_1) \\ k(x_2) \\ \vdots \\ k(x_N) \end{bmatrix} \quad (9)$$

The ELM's fundamental implementation employs the minimal non-linear least square approaches shown in eqn (10)

$$\alpha' = K^*O = K^T(KK^T)^{-1}O \quad (10)$$

Where  $K^* \rightarrow$  inverse of  $K \Rightarrow$  Moore–Penrose generalized inverse.

Additionally, the following equation can be used.

$$\beta' = K^T \left( \frac{1}{C} KK^T \right)^{-1} O \quad (11)$$

Consequently, the output function may be determined using the eqn above.

$$f_L(x) = k(x)\alpha = k(x)H^T \left( \frac{1}{C} KK^T \right)^{-1} O \quad (12)$$

## Section-4:

### 4.1 Experimentation

The entire experiment was run on an Intel I7 CPU with a 2GB NVIDIA GeForce K+10 GPU, 3GHZ, 16 GB RAM, and a 2TB hard. Utilizing Keras, the proposed architecture is put into practise (tensorflow as backend). The early stopping method was adopted to overcome the overfitting problem.

### 4.2 Performance Metrics :

Table2 Total No.of training and testing datasets for the presented approach (after augmentation)

S.no	Tot. Number of Images(Normal)	Training Data (Tr. %)	Testing Data (Ts. %)
01	14,836	70	30

Table 3 Number of overall Datasets (after Augmentation) (after Augmentation) utilised to test and train the suggested network

S.no	Tot. Number of Images(Tumor)	Training Data (Tr. %)	Testing Data (Ts. %)
01	34,948	70	30

The table displays the absolute number of datasets that were used to train and test the suggested illustration. Deep Feed-Forward layers using Extreme Learning machines are deployed for classification whose hyper-parameters employed in network training is listed in table 4

S.no	Hyper terms	Requisites
01	No of Epochs	300
02	No of Hidden Layers	200
03	Batch Size	40
04	Learning Rate	0.001

The experimentation involves the testing of the the proposed architecture in which the saliency segmented maps are used as the inputs to the feature layers and deep feed forward training networks that classifies the appropriate categories into normal and tumor. Metrics including accuracy (Acc), sensitivity (Sen), specificity (Spec), Precision (Pre), and f1-score are calculated to assess the effectiveness of the suggested design. Table 5 displays the computation formulas for the metrics used to evaluate the proposed architecture.

Table 5 Mathematical Equations for the calculation of specifications

S.NO	Specifications	Mathematical Equations
01	Accuracy (Acc)	$\frac{TP + TN}{TP + TN + FP + FN}$
02	Sensitivity (Sen)	$\frac{TP}{TP + FN} \times 100$

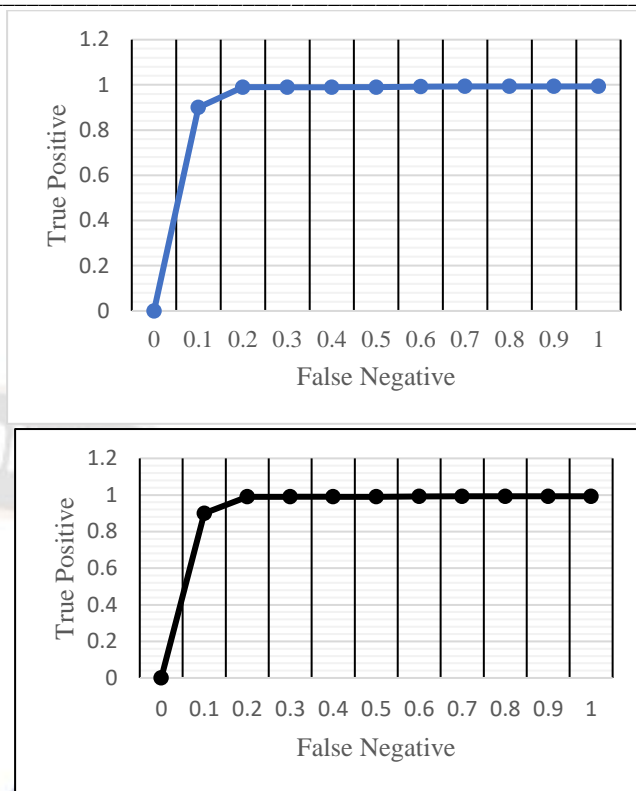


03	Specificity (Spec)	$\frac{TN}{TN + FP}$
04	Precision (Pre)	$\frac{TP}{TP + FP}$
05	F1-Score	$2 \cdot \frac{Precision * Recall1}{Precision + Recall1}$

Where, TP ⇒ True Positive Values,  
 TN ⇒ True Negative Values,  
 FP ⇒ False Positive  
 FN ⇒ False negative values

**4.3.1 RESULTS AND FINDINGS:**

This Section demonstrates the effectiveness of the other current models and the superiority of the proposed architecture. The suggested architecture's effectiveness is verified in three ways. In the first fold, confusion matrix is prone to validate the performance of the planned architecture. Additionally, ROC (Receiver operating characteristics) is applied for verifying the efficiency of the recommended architecture. Finally, the performance of the suggested architecture is compared with the other ongoing models. In order to address the imbalance issues, this suggested algorithm is evaluated on a random 1000 Kidney CT (50 percent normal, and 50 percent tumor-related) scan images.



(a) (b)  
 Figure 5 ROC curvature for the scheduled architecture in perceiving Normal and Other tumor stages from CT Kidney images.

CLASSES	Normal	Stone	Tumor	Cyst
Normal	98.22	0	1.2	0
Stone	1.2	98.3	0	1.2
Tumor	0	1.2	98.23	0
Cyst	0	0	1.6	98.35

Figure 6 Confusion Matrix employing 1000 randomly selected photos for the proposed architecture

Table 6 Comparison of the performance of the various algorithms with regard to Accuracy (Acc), sensitivity (Sen),

specificity (Spec), precision (Pre) and , F1 – score in predicting the Tumor Cancers in Kidney CT Images .

Algorithm Details	Specifications				
	Accuracy (Acc %)	Sensitivity (Sen %)	Specificity (Spec %)	Precision (Pre %)	F1-Score (%)
ADHCNN	80.2%	80.4%	81.0%	79.6%	80.4%
CNN-RF	83.3%	82.5%	81.5%	83%	81.7%
CNN-SVM	84.2%	83.67%	83.89%	83.27%	84.35%
CNN	78.4%	77.45%	76.74%	75.46%	75.78%
OPTIMISED CNN	91.02%	89.45%	88.0%	90.6%	89.78%
OPTIMISED LSTM	90.2%	89.2%	88.3%	88.36%	87.33%
CAPSNET	92.4%	91.62%	88.45%	88.4%	90.35%
Proposed Architecture	98.45%	98.2%	97.86%	98.2%	98.5%

Table 7 Performance of several deep learning architectures in predicting tumour cancers in kidney CT images, including accuracy, sensitivity, specificity, precision

Algorithm Details	Specifications				
	Accuracy (Acc %)	Sensitivity (Sen %)	Specificity (Spec %)	Precision (Pre %)	F1-Score (%)
ADHCNN	78.2%	78.23%	80.3%	79.46%	80.2%
CNN-RF	83.3%	82.5%	81.5%	83%	81.7%
CNN-SVM	83.3%	83.67%	83.89%	83.27%	84.35%
CNN	78.4%	77.45%	76.74%	75.46%	75.78%
OPTIMISED CNN	90.452%	90.45%	90.4%	89.46%	88.45%
OPTIMISED LSTM	89.4%	88.67%	88.34%	87.4%	86.33%
CAPSNET	92.4%	91.62%	88.45%	88.4%	90.35%
Proposed Architecture	98.45%	98.2%	97.86%	98.2%	98.5%

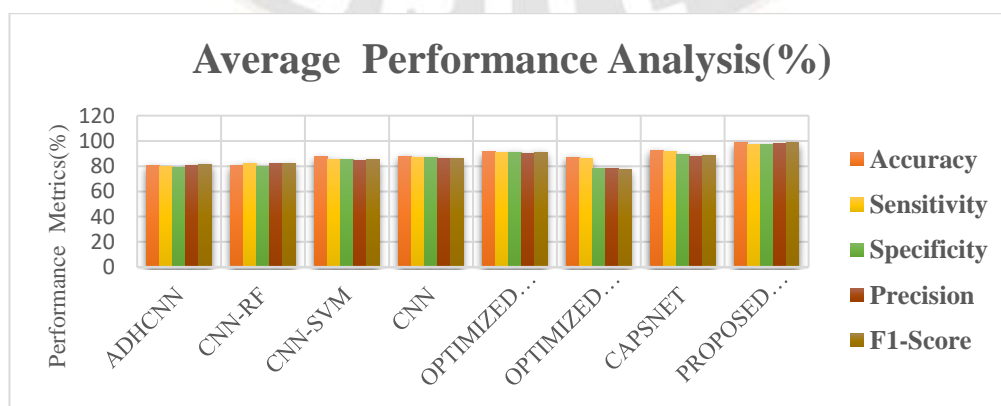


Figure 8 Comparative Analysis of Average Performance Metrics of different deep learning framework in forecasting the normal and tumor in kidney CT Images .



The confusion matrix (Figure 6) and ROC curve (Figure7) of the suggested framework for identifying the different types of CT scan Kidney visuals. The comparison of the performances of suggested and current algorithms is shown in Tables V and VI. According to Table 6, the suggested algorithm has demonstrated 98.4% accuracy in recognizing normal CT images with 98.5% sensitivity, 97.5% specificity, and a high f1score of 98.5%. From table VI, it can be shown that performance in identifying tumour photos was similar. From the tables 6 and 7, it is clear that fusion of saliency with U-NET and capsule networks in the proposed architecture has shown the better detection ratio. Additionally, experiments show that the suggested approach outperforms the other current algorithm. The average performance between the proposed and existing algorithms is compared in Figure 8 It is also obvious from Figure 8 that the suggested approach has outperformed the other algorithms that are currently in use.

## Section-5

### Conclusion and Future Enhancement:

The vital objective of this investigation is to find and categorize CT images such as Normal and Tumor cancer images using CT Scan Images .To accomplish this objective, the paper proposes the effective amalgamation of U-NET capsule networks with Deep Extreme Feed Forward layers. The proposed capsule U-NETs is used for segmentation whereas Deep extreme feed forward layers are used for the classification. The comprehensive experimentation has been conducted and evaluated the efficacy of the suggested illustration with the standard architectures. The outcome demonstrates that the suggested architecture surpassed other state-of-the-art architectures and achieved maximum results, including 98.4% accuracy, 97.8% sensitivity and specificity, 97.26% precision, and 98.5% F1-score. In the future, larger real-time clinical datasets will need to be used for more rigorous testing. Additionally, the suggested approach requires improvement in order to reduce computing overhead, which will be crucial for the timely diagnosis and effective treatment of kidney concerns in clinical settings.

### References :

- [1]. Abraham N, Khan NM. A novel focal tvsky loss function with improved attention u-net for lesion segmentation. In: 2019 IEEE 16th international symposium on biomedical imaging (ISBI 2019). IEEE; 2019. p. 683–7.
- [2]. Badrinarayanan V, Kendall A, Cipolla R. Segnet: a deep convolutional encoderdecoder architecture for image segmentation. *IEEE Trans Pattern Anal Mach Intell* 2017;39(12):2481–95
- [3]. Cairns P. Renal cell carcinoma. *Canc Biomarkers* 2011;9(1–6):461–73
- [4]. Christ PF, Ettliger F, Grün F, Elshaera MEA, Lipkova J, Schlecht S, Ahmaddy F, Tatavarty S, Bickel M, Bilic P, et al. Automatic liver and tumor segmentation of ct and mri volumes using cascaded fully convolutional neural networks. 2017. arXiv preprint arXiv:1702.05970.
- [5]. Çiçek O, € Abdulkadir A, Lienkamp SS, Brox T, Ronneberger O. 3d u-net: learning dense volumetric segmentation from sparse annotation. In: International conference on medical image computing and computer-assisted intervention. Springer; 2016. p. 424–32
- [6]. Dai J, Qi H, Xiong Y, Li Y, Zhang G, Hu H, Wei Y. Deformable convolutional networks. In: Proceedings of the IEEE international conference on computer vision; 2017. p. 764–73
- [7]. Fasihi MS, Mikhael WB. Overview of current biomedical image segmentation methods. In: 2016 international conference on computational science and computational intelligence (CSCI). IEEE; 2016. p. 803–8.
- [8]. Gillies RJ, Kinahan PE, Hricak H. Radiomics: images are more than pictures, they are data. *Radiology* 2016;278(2):563–77.
- [9]. Grana C, Borghesani D, Cucchiara R. Optimized block-based connected components labeling with decision trees. *IEEE Trans Image Process* 2010;19(6): 1596–609
- [10]. Hatamizadeh A, Terzopoulos D, Myronenko A. Boundary aware networks for medical image segmentation. 2019. arXiv preprint arXiv:1908.08071
- [11]. G. Chen et al., "Prediction of Chronic Kidney Disease Using Adaptive Hybridized Deep Convolutional Neural Network on the Internet of Medical Things Platform," in *IEEE Access*, vol. 8, pp. 100497-100508, 2020, doi: 10.1109/ACCESS.2020.2995310.
- [12]. N. Bhaskar and S. Manikandan, "A Deep-Learning-Based System for Automated Sensing of Chronic Kidney Disease," in *IEEE Sensors Letters*, vol. 3, no. 10, pp. 1-4, Oct. 2019, Art no. 7001904, doi: 10.1109/LESENS.2019.2942145.
- [13]. J. Qin, L. Chen, Y. Liu, C. Liu, C. Feng and B. Chen, "A Machine Learning Methodology for Diagnosing Chronic Kidney Disease," in *IEEE Access*, vol. 8, pp. 20991-21002, 2020, doi: 10.1109/ACCESS.2019.2963053.
- [14]. L. Antony et al., "A Comprehensive Unsupervised Framework for Chronic Kidney Disease Prediction," in *IEEE Access*, vol. 9, pp. 126481-126501, 2021, doi: 10.1109/ACCESS.2021.3109168.
- [15]. D. Pavithra and R. Vanithamani, "Chronic Kidney Disease Detection from Clinical Data using CNN," 2021 IEEE International Conference on Distributed Computing, VLSI, Electrical Circuits and Robotics (DISCOVER), 2021, pp. 282-285, doi: 10.1109/DISCOVER52564.2021.9663670.
- [16]. G. S. K. G. Prasad, A. A. Chowdari, K. P. Jona and R. Senapati, "Detection of CKD from CT Scan images using KNN algorithm and using Edge Detection," 2022 2nd International Conference on Emerging Frontiers in Electrical and Electronic Technologies (ICEFEET), 2022, pp. 1-4, doi: 10.1109/ICEFEET51821.2022.9848173.
- [17]. N. Bhaskar, M. Suchetha and N. Y. Philip, "Time Series Classification-Based Correlational Neural Network With Bidirectional LSTM for Automated Detection of Kidney

- Disease," in IEEE Sensors Journal, vol. 21, no. 4, pp. 4811-4818, 15 Feb.15, 2021, doi: 10.1109/JSEN.2020.3028738.
- [18]. S. Akter et al., "Comprehensive Performance Assessment of Deep Learning Models in Early Prediction and Risk Identification of Chronic Kidney Disease," in IEEE Access, vol. 9, pp. 165184-165206, 2021, doi: 10.1109/ACCESS.2021.3129491.
- [19]. D. Weerasinghe, B. T. G. S. Kumara, B. Kuhaneswaran and S. K. Gunathilake, "Identifying the Type of Chronic Kidney Disease Based on Heavy Metals in Soil using ANN," 2021 Third International Sustainability and Resilience Conference: Climate Change, 2021, pp. 270-274, doi: 10.1109/IEEECONF53624.2021.9667974.
- [20]. V. Shanmugarajeshwari and M. Ilayaraja, "Chronic Kidney Disease for Collaborative Healthcare Data Analytics using Random Forest Classification Algorithms," 2021 International Conference on Computer Communication and Informatics (ICCCI), 2021, pp. 1-14, doi: 10.1109/ICCCI50826.2021.9402574.
- [21]. Soo-Chang Pei; Yu-Zhe Hsiao," Spatial Affine transformations of images by using fractional shift fourier transform", 2015 IEEE International Symposium on Circuits and Systems (ISCAS), doi:<https://doi.org/10.1109/ISCAS.2015.7168951>
- [22]. Banerjee S, Mitra S, Shankar BU, Hayashi Y (2016) A novel GBM saliency detection model using multi-channel MRI. Plos one 11(1):e0146388
- [23]. Takacs P, Manno-Kovacs A (2018) Mri brain tumor segmentation combining saliency and convolutional network features. In: 2018 International conference on content-based multimedia indexing (CBMI), pp 1–6
- [24]. Ronneberger O, Fischer P, Brox T (2015) U-net: Convolutional networks for biomedical image segmentation. In: International conference on medical image computing and computer-assisted intervention. Springer, pp 234–241
- [25]. G.-B. Huang, Q.-Y. Zhu, and C.-K. Siew, "Extreme learning machine: theory and applications," Neurocomputing, vol. 70, no. 1, pp. 489–501, 2006.
- [26]. Wang B, Huang S, Qiu J, et al. Parallel online sequential extreme learning machine based on MapReduce. Neurocomputing 2015; 149: 224-32.